Plumbogaidonnayite, $PbZrSi_3O_9 \cdot 2H_2O$, a new Pb-member of the gaidonnayite group from the Saima alkaline complex, Liaoning Province, China

Bin Wu[1*], Xiangping Gu[2], Xin Gui[1], Christophe Bonnetti[1,3], Can Rao[4], Rucheng Wang[5], Jianjun Wan[1] and Wenlei Song[6]

[1]State Key Laboratory of Nuclear Resources and Environment, East China University of Technology, Nanchang, Jiangxi 330013, China

[2]School of Geosciences and Info-physics, Central South University, Changsha, Hunan 410083, China

[3]Arethuse Geology EURL, 29 Allée de Saint Jean, Fuveau 13710, France

[4]School of Earth Sciences, Zhejiang University, Hangzhou, Zhejiang 310027, China

[5]State Key Laboratory for Mineral Deposits Research, School of Earth Sciences and Engineering, Nanjing University, Nanjing, Jiangsu 210033, China

[6]State Key Laboratory of Continental Dynamics, Department of Geology, Northwest University, Xi'an, Shaanxi 710069, China

[*]E-mail: wubin@ecut.edu.cn (Bin Wu)

Mineralogical Society

This is a 'preproof' accepted article for Mineralogical Magazine. This version may be subject to change during the production process.
DOI: 10.1180/mgm.2024.2

Abstract

Plumbogaidonnayite, ideally $PbZrSi_3O_9 \cdot 2H_2O$, is a new gaidonnayite-group mineral discovered as a secondary product deriving from the alteration of eudialyte from the Saima alkaline complex, China. It occurs as aggregates (up to 1 mm) composed of subhedral to anhedral or platy crystals (individually 5–50 μm), closely associated with microcline, natrolite, aegirine, gaidonnayite, georgechaoite, zircon, bobtraillite, and britholite-(Ce) in eudialyte pseudomorph. The crystals are transparent, colorless or light brown with a vitreous lustre. Plumbogaidonnayite is brittle with conchoidal fracture, and it has a Mohs hardness of ~5 and a calculated density of 3.264 g/cm^3. It is optically biaxial (+) with α = 1.61(3), β = 1.63(3), and γ = 1.66(4). The calculated $2V$ is 80°, with the optical orientations X, Y, and Z parallel to the crystallographic a, b, and c axes, respectively. The empirical formula is $(Pb_{0.70}Ca_{0.17}Ba_{0.01}K_{0.11}Na_{0.01}Y_{0.01})_{\Sigma 1.01}(Zr_{1.00}Hf_{0.01}Ti_{0.01})_{\Sigma 1.02}Si_{3.01}O_9 \cdot 2H_2O$ calculated on the basis of nine oxygen atoms per formula unit and assuming the occurrence of two H_2O groups. Plumbogaidonnayite is orthorhombic, $P2_1nb$, a = 11.7690(4) Å, b = 12.9867(3) Å, c = 6.66165(16) Å, V = 1018.17(5) Å^3 and Z = 4. The nine strongest lines of its powder XRD pattern [d in Å (I, %) (hkl)] are: 6.489 (36) (020), 5.803 (100) (101), 4.661 (27) (021), 4.336 (29) (121), 3.640 (30) (221), 3.114 (79) (112), 2.947 (27) (400), 2.622 (27) (241), and 2.493 (27) (312). Plumbogaidonnayite has a similar spiral chain framework structure with gaidonnayite and georgechaoite, which is composed of SiO_4 tetrahedra and ZrO_6 octahedra, but with disordered extraframework sites (cations and H_2O groups) characterized by the substitution of $2Na^+$ (K^+)→Pb^{2+} (Ca^{2+}) + □ (vacancy). The discovery of plumbogaidonnayite adds a new perspective on the cation ordering and heterovalent substitution mechanism in gaidonnayite-group minerals.

https://doi.org/10.1180/mgm.2024.2 Published online by Cambridge University Press

Keywords: plumbogaidonnayite, new mineral, chain silicate mineral, microporous zirconosilicate, Saima alkaline complex

Introduction

Microporous materials with zeolitic structure, specifically titano- and zirconosilicates with complex octahedral-tetrahedral frameworks, have been extensively studied owing to their industrial properties (e.g., ion-exchange, sorption and catalysis) in modern technologies (Mumpton, 1999; Kuznicki *et al*., 2001; Celestian *et al*., 2019). Gaidonnayite-group minerals are hydrous zirconosilicates with microporous heteropolyhedral framework and so far only two natural types of alkali metal-dominant members, namely gaidonnayite ($Na_2ZrSi_3O_9 \cdot 2H_2O$) and georgechaoite ($KNaZrSi_3O_9 \cdot 2H_2O$), have been reported (Chao and Watkinson, 1974; Boggs and Ghose, 1985).

The new mineral plumbogaidonnayite $PbZrSr_3O_9 \cdot 2H_2O$, as the first divalent cation-dominant Pb member of the gaidonnayite group, was discovered in lujavrite from the Saima alkaline complex, Liaoning Province, China. This complex is also the type locality for fengchengite (IMA 2007-018a), hezuolinite (IMA 2010-045), and recently approved fluorsigaiite (IMA 2021-87a) and gysinite-(La) (IMA 2022-008, Yang *et al*., 2012; Shen *et al*., 2017; Wu *et al*., 2022, 2023a). The prefix "plumbo" was added to indicate its Pb-dominant compositional signature as suggested by the International Mineralogical Association, Commission on New Minerals, Nomenclature and Classification (IMA-CNMNC, Hatert and Burke, 2008). This new species with official name plumbogaidonnayite and symbol "Pgdn" have been approved by the IMA-CNMNC (IMA 2022-095, Wu *et al*., 2023b). The type material (catalogue number M16139) was deposited at the Geological Museum of China (No.

https://doi.org/10.1180/mgm.2024.2 Published online by Cambridge University Press

15 Yangrouhutong, Xisi, Beijing 100031, China). This paper aims to present the mineral paragenesis, chemical composition and crystal structure of plumbogaidonnayite, and compares its characteristics with other members of the gaidonnayite group.

Occurrence and origin

The Triassic Saima complex (220–230 Ma) is situated on the Liaodong Peninsula within the northeastern margin of the North China Craton, and its lujavrite hosts the typical alkaline rock-type Zr-REE-Nb mineralization (Wu *et al.*, 2016; Ma and Liu, 2023). The lujavrite with ~20% exposed area intruded the main body of nepheline syenite as sheets, stocks or dikes at the northeast and northwest edges of the complex. It is composed of predominant K-feldspar, nepheline, aegirine, and variable amounts of Zr-REE-Nb-bearing accessory minerals including zircon, eudialyte, pyrochlore, rinkite-(Ce), and wadeite (Wu *et al.*, 2016). Late metasomatism such as alkali-metasomatism, skarnification and carbonation prevailed through the whole Saima alkaline complex and led to the dissolution of precursor Zr-REE-Nb-bearing minerals (e.g., wadeite and eudialyte), and the precipitation of a series of secondary alteration minerals (e.g., natrolite, calcite, britholite-(Ce) and zircon, Wu *et al.*, 2015, 2018). The geological, mineralogical, and geochronological features of the Saima complex have been extensively reported in recent works (e.g., Wu *et al.*, 2010, 2016; Zhu *et al.,* 2016, 2017).

Plumbogaidonnayite occurs as subhedral to anhedral or platy crystals of ~5–50 μm across, commonly forming aggregates (up to 1 mm) in pseudomorph of altered eudialyte in Saima lujavrite (Fig. 1). It is closely associated with other secondary products after eudialyte alteration, including natrolite, aegirine, gaidonnayite,

https://doi.org/10.1180/mgm.2024.2 Published online by Cambridge University Press

georgechaoite, zircon, bobtraillite, and britholite-(Ce). Plumbogaidonnayite might be directly crystallized from eudialyte alteration, or more likely transformed from gaidonnayite or georgechaoite, which occur as the intermediate products after eudialyte alteration, by the natural ion exchange $2Na^{+}(K^{+}) \rightarrow Pb^{2+}(Ca^{2+}) + \square$ (vacancy) as reported in other microporous framework silicate minerals (e.g., vigrishinite and zvyaginite, Pekov and Chukanov, 2005; Pekov *et al.,* 2013, 2014). Of note, other hydrothermal Pb-bearing minerals like galena and gysinite-(La) were also observed in interstices of microcline in the plumbogaidonnayite-bearing lujavrite samples. The texture and mineral relationships indicate that lead in plumbogaidonnayite was likely derived from external Pb-rich hydrothermal fluids and zirconium from primary eudialyte dissolution (PbO < 1 wt.%, Wu *et al.,* 2016).

Physical and optical properties

Plumbogaidonnayite is transparent, colourless or light brown in transmitted light with a vitreous lustre. The streak color is white. It is brittle with conchoidal fracture, and no cleavage or twinning was observed. The Mohs hardness value is estimated at ~5 in analogy with other gaidonnayite-group minerals. The calculated density of plumbogaidonnayite is 3.264 g/cm^3 based on its unit-cell parameters and empirical formula (see below). Optically, it is biaxial (+) with α = 1.61(3), β = 1.63(3), and γ = 1.66(4) (white light). The calculated $2V$ is 80°, with optical orientation α//a, β//b, and γ//c. Some physical and optical properties could not be tested owing to the small crystal size. According to its measured refraction indices and calculated density, the compatibility index [1 – (K_P/K_C)] yields 0.053, which belongs to the "good" category (Mandarino, 1981).

https://doi.org/10.1180/mgm.2024.2 Published online by Cambridge University Press

Raman spectroscopy

Raman spectrum of plumbogaidonnayite was obtained using a Renishaw inVia RM2000 spectrometer at the State Key Laboratory of Nuclear Resources and Environment, East China University of Technology, China. Excitation wavelength and working power were set at 532 nm and 20 mW, respectively. Before collection, a pure silicon material (520 cm^{-1}) was selected for equipment calibration. In order to get a strong Raman signature and indicate the presence of H_2O, spectrum signals were collected from 100 to 4000 cm^{-1} with a 30 s accumulation time and 2-3 accumulations were adopted.

The Raman characteristics for structural framework in plumbogaidonnayite, which is composed of SiO_4 tetrahedra and ZrO_6 octahedra, are similar to those of gaidonnayite, georgechaoite and isostructural synthetic materials (Celestian *et al.*, 2019, Fig. 2). The strongest Raman band at 521 cm^{-1} is assigned to the symmetric stretching mode of the three-member ring formed by Si1-, Si2-, and Zr1-centered polyhedra (see Fig. 4), and band at 738 cm^{-1} probably represents the mixed vibrations of this ring (Sitarz *et al.*, 2000; Kovalskaya *et al.*, 2023). The second strongest band at 920 cm^{-1} is assigned to the stretching mode of [$Zr1O_6$]–[$Si2O_4$] spiral chain extending along *a*-axis. The moderate peak at 325 cm^{-1} possibly corresponds to SiO_4 ν_4 antisymmetric bending or lattice vibrations, and 687 cm^{-1} may represent the Si–O–Si bend involving the bridging oxygen. Weak band at 454 cm^{-1} can be assigned to lattice vibration and other weak bands from 900 to 1100 cm^{-1} (i.e., bands at 1011, 1034 and 1059 cm^{-1}) represent asymmetric Si–O stretching vibrations in SiO_4 tetrahedra, as illustrated in some other species, as for instance some zeolite-group minerals (Dutta and Del Barco, 1985). The bands of H_2O present at 3486 and 1612 cm^{-1}correspond to the symmetric O–H stretching mode and H–O–H bending mode, respectively (Carey

https://doi.org/10.1180/mgm.2024.2 Published online by Cambridge University Press

and Korenowski, 1998). In addition, broad bands at 2460 and 3065 cm^{-1} are probably assigned to SiO–H stretching vibrations or hydrogen bonds in potential hydrated H_3O^+ complexes, which widely exist in hydrous zirconosilicates (e.g., eudialyte-group minerals, Chukanov *et al.*, 2022; Kovalskaya *et al.*, 2023).

Chemical composition

Chemical composition of plumbogaidonnayite was determined using a JEOL-JXA 8530F Plus electron probe micro-analyzer (EPMA) in wavelength dispersive spectroscopy (WDS) mode at 15 kV and 50 nA at the State Key Laboratory of Nuclear Resources and Environment, East China University of Technology, China. A defocused beam (5 μm) was chosen for this hydrous mineral to minimise the element diffusion (e.g., K, Na and Ca). Counting times for stable elements on peaks and background were 20 and 10 s and those for K, Na and Ca were 10 and 5 s, respectively. Standards selected for calibration are listed in Table 1. Calculated on the basis of nine oxygen atoms and assuming the occurrence of two H_2O groups, 23 analyses on different plumbogaidonnayite grains give the following empirical chemical formula: $(Pb_{0.70}Ca_{0.17}Ba_{0.01}K_{0.11}Na_{0.01}Y_{0.01})_{\Sigma 1.01}(Zr_{1.00}Hf_{0.01}Ti_{0.01})_{\Sigma 1.02}Si_{3.01}O_9 \cdot 2H_2O$. The ideal formula of $PbZrSi_3O_9 \cdot 2H_2O$ requires PbO 39.68, ZrO_2 21.89, SiO_2 32.03, H_2O_{calc} 6.40, total 100 (all in wt.%). Some crystals show compositional heterogeneity under backscattered electron imaging due to variations in K (0.04–0.24 apfu), Ca (0.02–0.32 apfu) and Pb (0.62–0.80, Fig. 1c). Overall, Pb shows the negative relation with K, Na and Ca, implying potential $Pb^{2+} \rightarrow 2K^+(Na^+)$ and $Pb^{2+} \rightarrow Ca^{2+}$ substitutions in plumbogaidonnayite (Fig. 3).

https://doi.org/10.1180/mgm.2024.2 Published online by Cambridge University Press

Powder X-ray diffraction

The powder X-ray diffraction (XRD) of plumbogaidonnayite was collected at the School of Earth Sciences and Info-physics, Central South University, China, using a Rigaku XtaLAB Synergy diffractometer (Cu*K*α, λ = 1.54184 Å) in powder Gandolfi mode. Working voltage and current were set at 50 kV and 1 mA, respectively. The structural model of a single crystal (see below) was used to index the powder XRD pattern of plumbogaidonnayite (Table 2). The nine strongest lines [*d* in Å (*I*, %) (*hkl*)] are: 6.489 (36) (020), 5.803 (100) (101), 4.661 (27) (021), 4.336 (29) (121), 3.640 (30) (221), 3.114 (79) (112), 2.947 (27) (400), 2.622 (27) (241), and 2.493 (27) (312). Refined orthorhombic unit-cell parameters are: a = 11.7696(5) Å, b = 13.0048(4) Å, c = 6.6588(4) Å, V = 1019.21(5) Å, and Z = 4, which were obtained from the powder data handled by the software program *UnitCell* (Holland and Redfern, 1997).

Crystal structure determination

Single-crystal X-ray diffraction data were collected on the same diffractometer equipped with Cu*K*α radiation (λ = 1.54184 Å) at 50 kV and 1mA. Since the sample size is very small (20 μm or less), Cu*K*α was adopted due to its strong intensity to obtain good quality diffraction data for a X-ray tube of 50 W power. A relatively homogeneous plumbogaidonnayite crystal (20 × 20 × 20 μm) was dug from a polished thin section to perform a structure refinement. It contains (in wt.%) SiO_2 34.96–36.36, ZrO_2 23.52–24.90, HfO_2 0.26–0.48, Y_2O_3 0.02–0.55, CaO 1.84–2.74, PbO 28.55–31.63, Na_2O 0.01–0.11 and K_2O 0.43–1.07 based on eight analysis spots in and around the grain, yielding the average composition $(Pb_{0.69}Ca_{0.20}K_{0.10}Na_{0.01}Y_{0.02})_{\Sigma 1.03}(Zr_{1.00}Hf_{0.01})_{\Sigma 1.01}Si_{3.00}O_9 \cdot 2H_2O$. The software *CrysAlis*^{Pro} (Rigaku Oxford Diffraction, UK) and *SHELX* (Sheldrick, 2015a, b) were

https://doi.org/10.1180/mgm.2024.2 Published online by Cambridge University Press

used for diffraction data processing and structure refinement. The plumbogaidonnayite structure was solved in space group $P2_1nb$ and all sites were first refined with isotropic vibrations. The occupancies of Si, Zr and O were fixed at 1 and those for Pb, Ca, and K were freely refined. The result of $(Pb_{0.62}\square_{0.38})(Ca_{0.18}K_{0.14}Pb_{0.04}\square_{0.64})ZrSi_3O_{11}$ is consistent with the EPMA data. During the refinement, the splitting of Pb into Pb1, Pb2 and Pb3 subsites with low occupancy from the same site was necessary because an unsplit model, like those of gaidonnayite and georgechaoite, would lead to unreasonable results with R_1 = 9.04%, shift = 1.044 and a residual maximum = 7.2 eÅ^{-3} around Pb site (0.990 and 0.898 Å for Pb1–Pb2 and Pb1–Pb3 distances, respectively). In addition, the occupancy of Pb (Pb1, Pb2 and Pb3) site by Ca and K were also tested but it required too many Ca (0.62 *apfu*) and K (0.31 *apfu*) atoms due to electron density, which disagreed with the EPMA data. Similarly, Ca (Ca1, K1 and Pb4) site may also split due to its unusual displacement parameter (U_{eq} = 0.311 Å^2) in an unsplit model, thus, combined with residual electron densities and peaks around Ca site, we also make it split into Ca1, K1 and Pb4 subsites with much lower U_{eq} (0.073, 0.13 and 0.10 Å^2, respectively) by isotropic refinement. Anisotropic refinement for these subsites was also tried, but it made atoms nearly overlapped again like the unsplit model and led to a non-positive-definite result. The crystal structure refinement finally converged to R_1 = 5.59% for 1788 unique reflections (I>2σ(I)) and 182 parameters. Unit cell parameters refined are: a = 11.7690(4) Å, b = 12.9867(3) Å, c = 6.66165(16) Å, V = 1018.17(5) Å^3, Z = 4, and $P2_1nb$. Details for reflections collection and refinement are available in Table 3, and corresponding atom coordinates, site occupancies, equivalent isotropic and anisotropic atomic displacement parameters are provided in Tables 4 and 5. Selected bond distances and angles are given in Table 6, and bond-valence sums for each atom

https://doi.org/10.1180/mgm.2024.2 Published online by Cambridge University Press

are presented in Table 7. The structure of plumbogaidonnayite is shown in Fig. 4. The crystallographic information file has been deposited with the Principal Editor of *Mineralogical Magazine* and is available as Supplementary material (see below).

Plumbogaidonnayite is a new Pb-member of the gaidonnayite-group minerals containing similar zirconosilicate framework with gaidonnayite and georgechaoite (Chao, 1985; Ghose and Thakur, 1985). It is composed of sinusoidal six [SiO_4] tetrahedra-repeat single silicate chains extending along [101] and [$10\bar{1}$] (Fig. 4a), and then chains are corner-linked with [ZrO_6] octahedra into a three-dimensional framework. However, splitting and disordering occur at the extraframework sites (including cations and H_2O groups) in plumbogaidonnayite structure in the space between the silicate chains and [ZrO_6] octahedra, which are commonly fully ordered and occupied by Na and K in gaidonnayite and georgechaoite. Of note, the strong disorder in the extraframework sites would still lead to some physically unreasonable parameters related to these positions, which are assigned based on electron densities and statistical coordinates. For instance, the large U_{eq} values (0.126(13) and 0.146(15) $Å^2$) for H_2O groups may suggest the partial occupancy at the O10 and O11 sites. In addition, some short distances between extraframework sites, such as Pb2–O10 (2.09(3) Å), K1–O11 (1.47(14) Å), Pb1–Ca1 (2.24(5) Å), Pb2–Ca1 (2.33(5) Å), Pb3–Pb4 (2.29(9) Å), and Pb3–K1 (3.18(15) Å), could indicate the mutually exclusive occupancy of these two positions or potentially partial H_2O groups involved at these disordered cation sites.

Si–O tetrahedra

In plumbogaidonnayite, three crystallographically distinct Si1, Si2 and Si3 sites in SiO_4 tetrahedra are fully occupied by Si with average Si–O bond distances of 1.628

https://doi.org/10.1180/mgm.2024.2 Published online by Cambridge University Press

(Si1–O), 1.615 (Si2–O) and 1.614 (Si3–O) Å. These tetrahedra form a basic sinusoidal six [SiO_4] tetrahedra-repeat single $[Si_6O_{18}]^{12-}$ chain by corner-sharing (Fig. 4a). The Si–O–Si angles which involve bridging oxygen range from 133.0 to 135.2° with an average of 134.4°. The average bridging Si–O distance (1.629 Å) is longer than that of non-bridging Si–O bonds (1.608 Å), and average O–Si–O angle involving the bridging bonds (106.5°) is smaller than that with the non-bridging bonds (113.1°). These so-called "$^2T_6$ chains" and similar trends of Si–O bond and O–Si–O angle also exist in gaidonnayite, georgechaoite, stokesite and some synthetic materials (Day and Hawthorne, 2020 *and references therein*). The calculated bond-valence sum (BVS) for Si1 (4.04 v.u.), Si2 (4.20 v.u.) and Si3 (4.21 v.u.) are close to the ideal values within error (Table 7).

Zr–O octahedra

The Zr–O bond distances in relatively regular octahedra range from 2.056 to 2.154 Å with an average length of 2.094 Å. A single ZrO_6 octahedron is corner-linked with three different $[Si_6O_{18}]^{12-}$ chains by sharing two oxygen atoms within each chain. These ZrO_6 octahedra and SiO_4 tetrahedra form 7-member rings and 3-member rings from the view nearly along the *c*-axis (Fig. 4b), as also illustrated in other gaidonnayite-group minerals. The ZrO_6 octahedron in plumbogaidonnayite tends to link with disordered Pb (Pb1, Pb2 and Pb3) atoms via face- and edge-sharing, and with Ca (Ca1, K1 and Pb4) atoms via corner-sharing, while in gaidonnayite and georgechaoite structure it shares O–O edges with Na (K)–O octahedra (Chao, 1985; Ghose and Thakur, 1985).

Pb–O polyhedra

https://doi.org/10.1180/mgm.2024.2 Published online by Cambridge University Press

Pb in plumbogaidonnayite tends to occupy the Na2 site of the two Na sites in gaidonnayite, and it splits into three disordered Pb1, Pb2 and Pb3 sites with occupancies of 0.461(9), 0.099(7) and 0.057(9), respectively (Fig. 4c). Distances for Pb1–Pb2, Pb1–Pb3 and Pb2–Pb3 are 0.935(16), 0.88(5) and 1.23(5) Å, respectively. Pb1 is coordinated to three oxygen atoms (O1, O7 and O8) and two H_2O groups (O10 and O11), with three moderate Pb1–O bond lengths ranging from 2.396(14) to 2.661(14) Å and two Pb1–H_2O lengths of 2.30(4) and 2.67(3) Å, respectively. In contrast, Na–H_2O bonds are normally shorter than other Na–O bonds in Na–O octahedra in gaidonnayite and georgechaoite. The Pb1–O polyhedron shares a face (O1–O7–O8) with an adjacent ZrO_6 octahedron and a corner (O1) with an adjacent $Si1O_4$ tetrahedron. Pb2 is coordinated to four oxygen atoms (O1, O5, O7 and O9), and the Pb2–O polyhedron shares two edges (O5–O9 and O5–O7) with ZrO_6 octahedron and $Si2O_4$ tetrahedron, and two corners (O1 and O9) with $Si1O_4$ and $Si3O_4$ tetrahedra, respectively. The short Pb2–O10 distance of 2.09(3) Å may be a result of the statistically average positions of the extraframework atoms, or indicates the mutually exclusive occupancy of these two positions. Pb3 is coordinated to three oxygen atoms (O6, O7 and O9) and one H_2O molecule (O11) with an average length of 2.84 Å. The Pb3–O polyhedron shares oxygen (O6, O7 and O9) corners with adjacent ZrO_6 octahedron and SiO_4 (Si2 and Si3) tetrahedra.

Ca–O polyhedra

Ca in plumbogaidonnayite tends to occupy the Na1 site of the two Na sites in gaidonnayite, which splits into different Ca1, K1 and Pb4 subsites with occupancies of 0.18(4), 0.14(5) and 0.040(11), respectively (Fig. 4c). Distances for Ca1–K1, Ca1–Pb4 and K1–Pb4 bonds are 1.81(15), 0.87(7) and 0.95(16) Å, respectively. Ca1 is

https://doi.org/10.1180/mgm.2024.2 Published online by Cambridge University Press

bound to one oxygen atoms (O6) and one H_2O group (O10) with the distances of 2.79(5) Å and 2.83(5) Å. Four K1–O (O1, O3, O4 and O8) bonds range from 2.69(11) to 3.13(10) Å. K1–O polyhedron is corner-linked with $Si1O_4$, $Si3O_4$ tetrahedra and ZrO_6 octahedron, and also shares O3–O4 edge with $Si1O_4$ tetrahedron and O1–O8 edge with ZrO_6 octahedron, respectively. The short K1–O11 distance (1.47(14) Å) may indicate that these two atoms cannot be simultaneously occupied, or the possibility of H_2O groups at these disordered extraframework cations. Pb4–O polyhedron is corner-linked (O8) with $Si3O_4$ tetrahedron and ZrO_6 octahedron. Pb4–O8 bond distance (2.78(7) Å) is longer than Pb4–H_2O (O10 and O11) bonds (2.62(6) Å and 2.40(9) Å, respectively).

Implications

Plumbogaidonnayite is the first naturally discovered divalent cation-dominant member of the gaidonnayite-group minerals, which occurs closely associated with hydrothermal gaidonnayite and georgechaoite after eudialyte alteration. Actually, the latter two are common alteration products after eudialyte in peralkaline complexes and eudialyte dissolution experiments (Ivanyuk *et al.*, 2015; Borst *et al.*, 2016; Mikhailova *et al.*, 2022), whereas the absence of plumbogaidonnayite in most cases is probably attributed to lacking Pb-rich metasomatic fluids. In contrast, late Sr-Pb-rich fluid activity was pervasive in the Saima alkaline complex (Wu *et al.*, 2015, 2018), which resulted in the replacement of primary zirconosilicates (e.g., wadeite and eudialyte) by a variety of hydrothermal minerals including plumbogaidonnayite, calcite and strontianite, as well as the formation of newly approved fluorsigaiite and gysinite-(La) (Wu *et al.*, 2022, 2023a).

Ion exchange widely occurs in gaidonnayite-group minerals and similar

https://doi.org/10.1180/mgm.2024.2 Published online by Cambridge University Press

zirconosilicates (e.g., catapleiite- and hilairite-group minerals) under natural and experimental conditions (Pushcharovskii *et al*., 2002; Aksenov *et al*., 2016; Celestian *et al*., 2019). Recent experiment demonstrated that Cs^{+} could exchange at the extraframework cation (Na) site into gaidonnayite structure from room temperature to 95 °C (Celestian *et al*., 2019), which implies that plumbogaidonnayite could crystallize from eudialyte alteration or its alteration product (e.g., gaidonnayite and georgechaoite) in a naturally low temperature fluid environment. In comparison with isovalent substitution, heterovalent ion exchange in isomorphism would not only influence the main Raman vibrational features and unit-cell parameters, but also tends to cause more vacancies at the extraframework cation sites and decrease the symmetry, as demonstrated by $Na^{+}\rightarrow Ca^{2+}$ exchanges in calciocatapleiite and calciohilairite, $Na^{+}\rightarrow Zn^{2+}$ exchanges in vigrishinite and zvyaginite, and $Na^{+}\rightarrow Pb^{2+}$ exchange in plumbogaidonnayite (Pushcharovskii *et al*., 2002; Pekov *et al.,* 2013, 2014; Aksenov *et al*., 2016). However, although Ca occupies the Na1 site over other cations (except vacancy) during our plumbogaidonnayite structure refinement, the Ca-member of gaidonnayite has not been ever discovered in natural samples, probably due to compositional similarity to calciocatapleiite (Mandarino and Sturman, 1978; Ilyushin *et al*., 1981). Nevertheless, the discovery of plumbogaidonnayite draws attention to the heterovalent substitution and structural disordering in gaidonnayite-group minerals.

Acknowledgements

Professor Igor V. Pekov and two anonymous reviewers are sincerely appreciated for their constructive comments. Dr. Kai Qu is thanked for his generous help in crystal refinement. This study was financially supported by the National Natural Science

https://doi.org/10.1180/mgm.2024.2 Published online by Cambridge University Press

Foundation of China (Grant No. 42272087 and 42072054), and the Natural Science Foundation of Jiangxi Province, China (Grant No. 20224ACB213012, 20212BAB203003 and 20232BCJ23003).

Competing interests

The authors declare none.

References

Aksenov S.M., Portnov A.M., Chukanov N.V., Rastsvetaeva R.K., Nelyubina Y.N., Kononkova N.N. and Akimenko M.I. (2016) Ordering of calcium and vacancies in calcium catapleiite $CaZr[Si_3O_9]\cdot 2H_2O$. *Crystallography Reports*, **61**, 376–382.

Boggs R.C. and Ghose S. (1985) Georgechaoite $NaKZrSi_3O_9\cdot 2H_2O$, a new mineral species from Wind Mountain, New Mexico. *The Canadian Mineralogist*, **23**, 1–4.

Borst A.M., Friis H., Andersen T., Nielsen T.F.D., Waight T.E. and Smit M.A. (2016) Zirconosilicates in the kakortokites of the Ilímaussaq complex, South Greenland: Implications for fluid evolution and high-field-strength and rare-earth element mineralization in agpaitic systems. *Mineralogical Magazine*, **80**, 5–30.

Brese N.E. and O'Keeffe M. (1991) Bond-valence parameters for solids. *Acta Crystallographica*, **B47**, 192–197.

Carey D.M. and Korenowski G.M. (1998) Measurement of the Raman spectrum of liquid water. *Journal of Chemical Physics*, **108**, 2669–2675.

Celestian A.J., Lively J. and Xu W.Q. (2019) In situ Cs and H exchange into gaidonnayite and proposed mechanisms of ion diffusion. *Inorganic Chemistry*,

https://doi.org/10.1180/mgm.2024.2 Published online by Cambridge University Press

58, 1911−1928.

Chao G.Y. (1985) The crystal structure of gaidonnayite $Na_2ZrSi_3O_9 \cdot 2H_2O$. *The Canadian Mineralogist*, **23**, 11–15.

Chao G.Y. and Watkinson D.H. (1974) Gaidonnayite, $Na_2ZrSi_3O_9 \cdot 2H_2O$, a new mineral from Mont St. Hilaire, Quebec. *The Canadian Mineralogist*, **12**, 316–319.

Chukanov N.V., Vigasina M.F., Rastsvetaeva R.K., Aksenov S.M., Mikhailova J.A. and Pekov I.V. (2022) The evidence of hydrated proton in eudialyte-group minerals based on Raman spectroscopy data. *Journal of Raman Spectroscopy*, **53**, 1188–1203.

Day M.C. and Hawthorne F.C. (2020) A structure hierarchy for silicate minerals: chain, ribbon, and tube silicates. *Mineralogical Magazine*, **84**, 165–244.

Dutta P.K. and Del Barco B. (1985) Raman spectroscopic studies of zeolite framework. Hydrated zeolite and the influence of cations. *The Journal of Physical Chemistry*, **89**, 1861–1865.

Flack H.D. (1983). On enantiomorph-polarity estimation. *Acta Crystallographica*, **A39**, 876–881.

Ghose S. and Thakur P. (1985) The crystal structure of georgechaoite $NaKZrSi_3O_9 \cdot 2H_2O$. *The Canadian Mineralogist*, **23**, 5–10.

Hatert F. and Burke E.A.J. (2008) The IMA-CNMNC dominant-constituent rule revisited and extended. *The Canadian Mineralogist*, **46**, 717–728.

Holland T.J.B. and Redfern S.A.T. (1997) Unit cell refinement from powder

https://doi.org/10.1180/mgm.2024.2 Published online by Cambridge University Press

diffraction data: the use of regression diagnostics. *Mineralogical Magazine*, **61**, 65–77.

Ilyushin G.D., Voronkov A.A., Ilyukhin V.V., Nevskii N.N. and Belov N.V. (1981) Crystal structure of natural monoclinic catapleiite, $Na_2ZrSi_3O_9 \cdot 2H_2O$. *Doklady Akademii Nauk SSSR*, **260**, 623–627.

Ivanyuk G.Y., Pakhomovsky Y.A. and Yakovenchuk V.N. (2015) Eudialyte-group minerals in rocks of Lovozero layered complex at Mt. Karnasurt and Mt. Kedykvyrpakhk. *Geology of Ore Deposits*, **57**, 600–613.

Kovalskaya T.N., Ermolaeva V.N., Chukanov N.V., Varlamov D.A., Kovalskiy G.A., Zakharchenko E.S., Kalinin G.M. and Chaichuk K.D. (2023) Syethesis of Fe-deficient eudialyte analogues: Relationships between the composition of the reaction system and crystal-chemical features of the products. *Mineralogical Magazine*, **87**, 233−240.

Kuznicki S.M., Bell V. A., Nair S., Hillhouse H. W., Jacubinas R. M., Braunbarth C.M., Toby B. H. and Tsapatsis M. A. (2001) Titanosilicate molecular sieve with adjustable pores for size-selective adsorption of molecules. *Nature*, **412**, 720−724.

Ma D.Z. and Liu Y. (2023) Nb mineralization in the nepheline syenite in the Saima area of the North China Craton, China. *Ore Geology Reviews*, **152**, 105247.

Mandarino J.A. (1981) The Gladstone-Dale relationship: part IV. The compatibility concept and its application. *The Canadian Mineralogist*, **19**, 441–450.

Mandarino J.A. and Sturman B.D. (1978) The identity of α-catapleiite and

https://doi.org/10.1180/mgm.2024.2 Published online by Cambridge University Press

gaidonnayite. *The Canadian Mineralogist*, **16**, 195–198.

Mikhailova J.A., Pakhomovsky Y.A., Kalashnikova G.O. and Aksenov S.M. (2022) Dissolution of the eudialyte-group minerals: experimental modeling of natural processes. *Minerals*, **12**, 1460.

Momma K. and Izumi F. (2011) VESTA 3 for three-dimensional visualization of crystal, volumetric and morphology data. *Journal of Applied Crystallography*, **44**, 1272–1276.

Mumpton F. A. (1999) La roca magica: uses of natural zeolites in agriculture and industry. *Proceedings of the National Academy of Science*, **96**, 3463−3470.

Pekov I.V. and Chukanov N.V. (2005) Microporous framework silicate minerals with rare and transition elements: minerogenetic aspects. *Reviews in Mineralogy & Geochemistry*, **57**, 145–171.

Pekov I.V., Britvin S.N., Zubkova N.V., Chukanov N.V., Bryzgalov I.A., Lykova I.S., Belakovskiy D.I. and Pushcharovsky D.Y. (2013) Vigrishinite, $Zn_2Ti_{4-x}Si_4O_{14}(OH,H_2O,\square)_8$, a new mineral from the Lovozero alkaline complex, Kola Peninsula, Russia. *Geology of Ore Deposits*, **55**, 575–586.

Pekov I.V., Lykova I.S., Chukanov N.V., Yapaskurt V.O., Belakovskiy D.I., Zolotarev A.A., Jr. and Zubkova N.V. (2014) Zvyaginite $NaZnNb_2Ti[Si_2O_7]_2O(OH,F)_3(H_2O)_{4+x}$ ($x < 1$), a new mineral of the epistolite group from the Lovozero alkaline pluton, Kola peninsula, Russia. *Geology of Ore Deposits*, **56**, 644–656.

Pushcharovskii D.Y., Pekov I.V., Pasero M., Gobechiya E.R., Merlino S. and Zubkova

https://doi.org/10.1180/mgm.2024.2 Published online by Cambridge University Press

N.V. (2002) Crystal structure of cation-deficient calciohilairite and possible mechanisms of decationization in mixed-framework minerals. *Crystallography Reports*, **47**, 748–752.

Sheldrick G.M. (2015a) SHELXT – Integrated space-group and crystal structure determination. *Acta Crystallographica*, **A71**, 3–8.

Sheldrick G.M. (2015b) Crystal structure refinement with SHELX. *Acta Crystallographica*, **C71**, 3–8.

Shen G.F., Xu J.S., Yao P. and Li G.W. (2017) Fengchengite: a new species with the Na-poor but vacancy-dominant *N*(5) site in the eudialyte group. *Acta Mineralogica Sinica*, **37**, 140–151 (in Chinese with English abstract).

Sitarz M., Handke M. and Mozgawa W. (2000) Identification of silicooxygen rings in SiO2 based on IR spectra. *Spectrochimica Acta*, **A56**, 1819–1823.

Warr L.N. (2021) IMA-CNMNC approved mineral symbols. *Mineralogical Magazine*, **85**, 291–320.

Wu B., Gu X.P., Rao C., Wang R.C., Xing X.Q., Zhong F.J., Wan J.J. and Bonnetti C. (2022) Fluorsigaiite, $Ca_2Sr_3(PO_4)_3F$, a new mineral of the apatite supergroup from the Saima alkaline complex, Liaoning Province, China. *Mineralogical Magazine*, **86**, 940–947.

Wu B., Gu X.P., Rao C., Wang R.C., Xing X.Q., Wan J.J., Zhong F.J. and Bonnetti C. (2023a) Gysinite-(La), $PbLa(CO_3)_2(OH)\cdot H_2O$, a new rare earth mineral of the ancylite group from the Saima alkaline complex, Liaoning Province, China. *Mineralogical Magazine*, **87**, 143–150.

https://doi.org/10.1180/mgm.2024.2 Published online by Cambridge University Press

Wu B., Gu X.P., Rao C., Wang R.C., Xing X.Q., Wan J.J. and Zhong, F.J. (2023b) Plumbogaidonnayite, IMA 2022-095. CNMNC Newsletter 71, *European Journal of Mineral*ogy, **35**, 75-79.

Wu B., Gu X.P., Wang R.C., Liu X.C., Xing X.Q., and Ren Q. (2023c) Discovery and genesis of three critical metal-bearing minerals. *Geological Review*, **69**, https://doi.org/10.16509/j.georeview.2023.s1.083 (in Chinese).

Wu B., Wang R.C., Yang J.H., Wu F.Y., Zhang W.L., Gu X.P. and Zhang A.C. (2015) Wadeite ($K_2ZrSi_3O_9$), an alkali-zirconosilicate from the Saima agpaitic rocks in northeastern China: its origin and response to multi-stage activities of alkaline fluids. *Lithos*, **224–225**, 126–142.

Wu B., Wang R.C., Yang J.H., Wu F.Y., Zhang W.L., Gu X.P. and Zhang A.C. (2016) Zr and REE mineralization in sodic lujavrite from the Saima alkaline complex, northeastern China: A mineralogical study and comparison with potassic rocks. *Lithos*, **262**, 232–246.

Wu B., Wang R.C., Liu X.D., Guo G.L. and Song Z.T. (2018) Chemical composition and alteration assemblages of eudialyte in the Saima alkaline complex, Liaoning Province, and its implication for alkaline magmatic–hydrothermal evolution. *Acta Petrologica Sinica*, **6**, 1741–1757 (in Chinese with English abstract).

Wu F.Y., Yang Y.H., Marks M.A.W., Liu Z.C., Zhou Q., Ge W.C., Yang J.S., Zhao Z.F., Mitchell R.H. and Markl G. (2010) In situ U–Pb, Sr, Nd and Hf isotopic analysis of eudialyte by LA-(MC)-ICP-MS. *Chemical Geology*, **273**, 8–34.

Yang Z.M., Giester G., Ding K.S. and Tillmanns E. (2012) Hezuolinite,

https://doi.org/10.1180/mgm.2024.2 Published online by Cambridge University Press

$(Sr,REE)_4Zr(Ti,Fe^{3+},Fe^{2+})_2Ti_2O_8(Si_2O_7)_2$, a new mineral species of the chevkinite group from Saima alkaline complex, Liaoning Province, NE China. *European Journal of Mineralogy*, **24**, 189–196.

Zhu Y.S., Yang J.H., Sun J.F., Zhang J.H. and Wu F.Y. (2016) Petrogenesis of coeval silica-saturated and silica-undersaturated alkaline rocks: Mineralogical and geochemical evidence from the Saima alkaline complex, NE China. *Journal of Asian Earth Sciences*, **117**, 184–207.

Zhu Y.S., Yang J.H., Sun J.F. and Wang H. (2017) Zircon Hf-O isotope evidence for recycled oceanic and continental crust in the sources of alkaline rocks. *Geology*, **45**, 407–410.

https://doi.org/10.1180/mgm.2024.2 Published online by Cambridge University Press

Table and figure captions

Table 1. Chemical electron microprobe data (in wt.%) for plumbogaidonnayite.

Constituent	Mean	Range	Sd (σ)	Apfu	Standard
SiO_2	35.34	34.47-36.83	0.57	3.005	Zircon
TiO_2	0.13	0.02-0.29	0.09	0.008	Rutile
ZrO_2	24.09	22.79-25.56	0.55	1.000	Zircon
HfO_2	0.36	0.18-0.62	0.10	0.009	Hf metal
Y_2O_3	0.16	Bdl-0.55	0.15	0.007	Synthetic YPO_4
CaO	1.86	0.16-3.58	1.22	0.168	Plagioclase
BaO	0.20	0.05-0.35	0.07	0.007	Baryte
PbO	30.52	27.81-34.09	1.55	0.699	Crocoite
Na_2O	0.07	Bdl-0.18	0.04	0.012	Jadeite
K_2O	1.03	0.35-2.22	0.60	0.113	Orthoclase
H_2O^*	7.06	6.89-7.36	0.11	2.000	
Total	100.82	100.14-101.53	0.43		

Sd = standard deviation; Bdl = below detection limits; Apfu = atoms per formula unit.

*H_2O was assumed as 2 apfu according to the ideal formula of plumbogaidonnayite.

https://doi.org/10.1180/mgm.2024.2 Published online by Cambridge University Press

Table 2. Measured and calculated* powder X-ray diffraction data (*d* in Å, *I* in %) for plumbogaidonnayite.

I_{meas}	I_{calc}	D_{meas}	d_{calc}	*h k l*
36	**100**	**6.489**	**6.493**	**0 2 0**
100	**42**	**5.803**	**5.797**	**1 0 1**
9	7	5.309	5.294	1 1 1
27	**40**	**4.661**	**4.650**	**0 2 1**
29	**34**	**4.336**	**4.326**	**1 2 1**
24	17	4.181	4.176	2 1 1
30	**29**	**3.640**	**3.648**	**2 2 1**
21	24	3.469	3.469	1 3 1
17	15	3.361	3.358	3 2 0
9	2	3.242	3.271	3 1 1
79	**47**	**3.114**	**3.111**	**1 1 2**
27	**28**	**2.947**	**2.942**	**4 0 0**
11	2	2.825	2.829	2 1 2
15	11	2.659	2.664	3 3 1
27	**24**	**2.622**	**2.615**	**2 4 1**
1	4	2.569	2.576	1 3 2
27	**17**	**2.493**	**2.492**	**3 1 2**
1	2	2.415	2.409	2 3 2
3	3	2.367	2.370	1 5 1
3	2	2.284	2.281	1 4 2
8	7	2.217	2.219	5 0 1
7	14	2.167	2.164	0 6 0
4	5	2.103	2.100	5 2 1
14	12	2.052	2.051	2 1 3
4	3	2.030	2.028	1 6 1
12	6	1.967	1.965	4 3 2
6	5	1.946	1.943	2 6 1
2	2	1.904	1.896	3 6 0
3	4	1.863	1.862	6 1 1
4	3	1.810	1.807	6 2 1
6	2	1.761	1.765	3 3 3
9	5	1.748	1.744	4 6 0
2	2	1.710	1.710	2 7 1
8	2	1.684	1.687	5 5 1
8	4	1.627	1.628	6 4 1
1	3	1.609	1.606	1 7 2
5	3	1.569	1.563	1 8 1
1	1	1.550	1.550	5 6 1
2	1	1.513	1.513	5 3 3

https://doi.org/10.1180/mgm.2024.2 Published online by Cambridge University Press

7	3	1.494	1.498	3 7 2
3	1	1.462	1.461	6 1 3
7	2	1.419	1.421	4 8 0
4	3	1.386	1.384	2 7 3
3	2	1.372	1.372	5 5 3

*The calculated values were obtained using VESTA 3(Momma and Izumi, 2011).

The strongest values are given in bold.

https://doi.org/10.1180/mgm.2024.2 Published online by Cambridge University Press

Table 3. Data collection and structure refinement details for plumbogaidonnayite.

Crystal data	
Ideal formula	$PbZrSi_3O_9 \cdot 2H_2O$
Crystal dimensions (mm)	0.020 × 0.020 × 0.020
Crystal system, space group	Orthorhombic, $P2_1nb$
Temperature (K)	293(2)
a, b, c (Å)	11.7690(4), 12.9867(3), 6.66165(16)
V (Å^3)	1018.17(5)
Z	4
Calculated density (g·cm^{-3})	3.264
Data collection	
Crystal description	Colourless platy crystal
Working voltage (kV) and current (mA)	50, 1
Instrument	Rigaku XtaLAB Synergy
Radiation type, wavelength (Å)	Cu*K*α, 1.54184
Absorption coefficient, μ (mm^{-1})	34.716
F(000)	921
θ range (°)	6.818 to 77.55
No. of measured, independent and observed [$I > 2\sigma(I)$] reflections	5989, 1859, 1788
R_{int}	0.0554
Indices range of *h, k, l*	$-14 \leqslant h \leqslant 14$, $-16 \leqslant k \leqslant 12$, $-8 \leqslant l \leqslant 8$
Refinement	
Refinement	Full-matrix least squares on F^2
Number of reflections, restraints, parameters	1859, 1, 182
R_1 [$I > 2\sigma(I)$], R_1(all)	0.0559, 0.0576
wR_2 [$I > 2\sigma(I)$], wR_2(all)*	0.1345, 0.1355
GoF	1.114
Δρmax, Δρmin (*e* Å^{-3})	1.29, -1.17
Flack parameter#	0.072(12)

*$wR_2 = \{\sum[w(F_o^2-F_c^2)^2]/\sum[w(F_o^2)^2]\}^{1/2}$; $w = 1/[\sigma^2(F_o)^2 + (aP)^2 + bP]$ where *a* is 0.0454, *b* is 17.9195 and *P* is $[2F_c^2 + \mathrm{Max}(F_o^2, 0)]/3$.

#Flack parameter is calculated from Flack (1983).

https://doi.org/10.1180/mgm.2024.2 Published online by Cambridge University Press

Table 4. Wyckoff positions, atom coordinates, inferred site occupancies, and equivalent isotropic displacement parameters in plumbogaidonnayite structure.

Atom	*Wyck.*	*x*	*y*	*z*	Site occupancy	$U_{(eq)}$
Pb1	4*a*	0.9642(2)	0.06272(19)	0.6546(4)	$Pb_{0.461(9)}$	0.0352(11)
Pb2	4*a*	0.0071(10)	0.0776(6)	0.769(3)	$Pb_{0.099(7)}$	0.045(5)
Pb3	4*a*	0.025(4)	0.029(3)	0.614(6)	$Pb_{0.057(9)}$	0.101(17)
Ca1	4*a*	0.593(4)	0.063(3)	0.390(7)	$Ca_{0.18(4)}$	0.073(18)
K1	4*a*	0.722(12)	0.138(9)	0.404(14)	$K_{0.14(5)}$	0.13(5)
Pb4	4*a*	0.649(6)	0.107(5)	0.393(7)	$Pb_{0.040(11)}$	0.10(2)
Zr1	4*a*	0.24999(13)	0.06308(10)	0.13398(18)	Zr	0.0206(5)
Si1	4*a*	0.7279(4)	0.2051(4)	0.8832(6)	Si	0.0253(11)
Si2	4*a*	0.5098(5)	0.0842(3)	0.8943(6)	Si	0.0212(9)
Si3	4*a*	0.3026(4)	0.1173(3)	0.6379(6)	Si	0.0197(9)
O1	4*a*	0.2968(12)	-0.0970(9)	0.1520(17)	O	0.026(3)
O2	4*a*	0.5944(12)	0.1808(10)	0.932(2)	O	0.034(3)
O3	4*a*	0.7775(12)	0.2618(9)	0.0825(16)	O	0.029(3)
O4	4*a*	0.7321(11)	0.2820(8)	0.6932(17)	O	0.025(3)
O5	4*a*	0.5797(11)	-0.0196(9)	0.8603(19)	O	0.029(3)
O6	4*a*	0.4367(11)	0.1096(10)	0.6922(17)	O	0.030(3)
O7	4*a*	0.4250(11)	0.0725(10)	0.0827(19)	O	0.029(3)
O8	4*a*	0.2829(13)	0.0485(9)	0.4453(17)	O	0.031(3)
O9	4*a*	0.2282(11)	0.0848(10)	0.8307(14)	O	0.024(3)
O10 (H_2O)	4*a*	0.018(3)	0.231(2)	0.866(5)	O	0.126(13)
O11 (H_2O)	4*a*	0.844(4)	0.1524(19)	0.448(5)	O	0.146(14)

https://doi.org/10.1180/mgm.2024.2 Published online by Cambridge University Press

Table 5. Anisotropic displacement parameters (in Å^2) for plumbogaidonnayite.

Atom	U^{11}	U^{22}	U^{33}	U^{23}	U^{13}	U^{12}
Pb1	0.0340(17)	0.0379(13)	0.0337(15)	0.0074(8)	0.0071(11)	-0.0045(10)
Pb2	0.034(6)	0.036(5)	0.065(11)	0.000(4)	0.010(7)	-0.004(4)
Pb3	0.08(3)	0.13(3)	0.09(2)	0.04(2)	0.01(2)	0.03(2)
Zr1	0.0242(8)	0.0240(7)	0.0135(6)	-0.0026(5)	0.0019(6)	-0.0057(6)
Si1	0.027(3)	0.029(2)	0.0196(19)	-0.0018(16)	-0.0002(19)	-0.0036(18)
Si2	0.020(2)	0.026(2)	0.0176(19)	-0.0017(16)	-0.0002(18)	-0.0004(18)
Si3	0.026(2)	0.0237(19)	0.0096(16)	-0.0010(15)	0.0006(17)	0.0022(17)
O1	0.033(6)	0.022(5)	0.023(5)	0.005(4)	-0.003(5)	0.007(5)
O2	0.031(7)	0.034(6)	0.036(7)	-0.005(5)	-0.006(6)	-0.006(5)
O3	0.045(9)	0.023(5)	0.018(5)	0.009(4)	-0.002(5)	-0.005(5)
O4	0.033(7)	0.015(5)	0.027(5)	0.000(4)	0.005(5)	0.001(5)
O5	0.027(6)	0.028(6)	0.031(7)	-0.007(5)	-0.002(5)	0.010(5)
O6	0.032(7)	0.043(7)	0.016(5)	-0.001(5)	0.010(5)	0.002(6)
O7	0.026(7)	0.040(7)	0.023(6)	0.001(5)	0.005(6)	0.001(5)
O8	0.049(8)	0.034(6)	0.010(5)	0.002(4)	0.003(5)	-0.008(6)
O9	0.028(7)	0.042(7)	0.003(4)	-0.003(4)	0.003(5)	-0.011(5)
O10 (H_2O)	0.077(19)	0.096(18)	0.21(4)	-0.017(19)	0.04(2)	0.016(16)
O11 (H_2O)	0.23(4)	0.056(14)	0.15(3)	-0.060(16)	-0.03(3)	0.017(19)

https://doi.org/10.1180/mgm.2024.2 Published online by Cambridge University Press

Table 6. Selected bond distances (Å) and angles (°) for plumbogaidonnayite.

Si–O tetrahedra						in Si–O tetrahedra		Zr–O octahedra	
Si1–O1	1.638(14)	Si2–O2	1.621(13)	Si3–O3	1.640(12)	O–Si1–O^{mean}	109.4	Zr1–O1	2.154(11)
–O2	1.636(15)	–O5	1.595(12)	–O6	1.622(14)	O–Si2–O^{mean}	109.5	–O4	2.061(10)
–O3	1.626(12)	–O6	1.631(13)	–O8	1.581(13)	O–Si3–O^{mean}	109.4	–O5	2.082(13)
–O4	1.613(12)	–O7	1.611(14)	–O9	1.611(11)	between Si–O tetrahedra		–O7	2.092(13)
mean	1.628		1.615		1.614	Si1–O2–Si2	135.1(9)	–O8	2.118(11)
						Si1–O3–Si3	133.0(7)	–O9	2.056(9)
						Si2–O6–Si3	135.2(8)	mean	2.094

Pb–O polyhedra				Ca–O polyhedra				Cation distances	
Pb1–O1	2.396(14)	Pb3–O6	2.91(5)	Ca1–O6	2.79(5)	Pb4–O8	2.78(7)	Pb1–Pb2	0.935(16)
–O7	2.522(13)	–O7	2.68(4)	–O10	2.83(5)	–O10	2.62(6)	Pb1–Pb3	0.88(5)
–O8	2.661(14)	–O9	2.89(5)			–O11	2.40(9)	Pb2–Pb3	1.23(5)
–O10	2.67(3)	–O11	2.89(6)	mean	2.81	mean	2.60	Ca1–K1	1.81(15)
–O11	2.30(4)							Ca1–Pb4	0.87(7)
mean	2.510	mean	2.84					K1–Pb4	0.95(16)
Pb2–O1	2.542(18)			K1–O1	3.13(10)				

Mineralogical Society
This is a 'preproof' accepted article for Mineralogical Magazine. This version may be subject to change during the production process.
DOI: 10.1180/mgm.2024.2

–O5	2.72(2)	–O3	2.76(10)
–O7	2.388(16)	–O4	2.69(11)
–O9	2.637(18)	–O8	2.72(10)
–O10	2.09(3)	–O10	2.96(12)
mean	2.475	mean	2.85

Table 7. Calculated bond valence sums (in v.u.) of atoms for plumbogaidonnayite.*

	Zr1	Si1	Si2	Si3	Pb (Pb1, Pb2, Pb3)	Ca (Ca1, K1, Pb4)	Total
O1	$0.56^{\times1\downarrow1\rightarrow}$	$0.98^{\times1\downarrow1\rightarrow}$			$0.32^{\times1\downarrow1\rightarrow}$		1.86
O2		$0.99^{\times1\downarrow1\rightarrow}$	$1.03^{\times1\downarrow1\rightarrow}$				2.02
O3		$1.02^{\times1\downarrow1\rightarrow}$		$0.98^{\times1\downarrow1\rightarrow}$			2.00
O4	$0.72^{\times1\downarrow1\rightarrow}$	$1.05^{\times1\downarrow1\rightarrow}$					1.77
O5	$0.68^{\times1\downarrow1\rightarrow}$		$1.11^{\times1\downarrow1\rightarrow}$		$0.03^{\times1\downarrow1\rightarrow}$		1.82
O6			$1.00^{\times1\downarrow1\rightarrow}$	$1.03^{\times1\downarrow1\rightarrow}$		$0.02^{\times1\downarrow1\rightarrow}$	2.05
O7	$0.66^{\times1\downarrow1\rightarrow}$		$1.06^{\times1\downarrow1\rightarrow}$		$0.27^{\times1\downarrow1\rightarrow}$	$0.02^{\times1\downarrow1\rightarrow}$	2.01
O8	$0.61^{\times1\downarrow1\rightarrow}$			$1.14^{\times1\downarrow1\rightarrow}$	$0.14^{\times1\downarrow1\rightarrow}$	$0.05^{\times1\downarrow1\rightarrow}$	1.94
O9	$0.73^{\times1\downarrow1\rightarrow}$			$1.06^{\times1\downarrow1\rightarrow}$	$0.03^{\times1\downarrow1\rightarrow}$	$0.03^{\times1\downarrow1\rightarrow}$	1.85
O10 (H_2O)					$0.27^{\times1\downarrow1\rightarrow}$	$0.06^{\times1\downarrow1\rightarrow}$	0.33
O11 (H_2O)					$0.37^{\times1\downarrow1\rightarrow}$	$0.07^{\times1\downarrow1\rightarrow}$	0.44
Total	3.96	4.04	4.20	4.21	1.43	0.25	

* Bond valence sums were calculated with the site occupancy given in Table 4, using the parameters of Brese and O'Keeffe (1991).

https://doi.org/10.1180/mgm.2024.2 Published online by Cambridge University Press

Fig. 1. Photomicrograph (a) and backscattered electron images (b-d) showing the occurrence of plumbogaidonnayite. (a-b) Plumbogaidonnayite aggregate as an alteration product in pseudomorph after eudialyte. (c-d) Plumbogaidonnayite grains (including holotype crystal selected for Raman spectroscopy and single XRD determination) associated with other secondary minerals including gaidonnayite, natrolite, and britholite-(Ce) and eudialyte relics. Mineral abbreviations after Warr (2021): Ab – albite, Aeg – aegirine, Bri-Ce – britholite-(Ce), Eud – eudialyte, Gdn – gaidonnayite, Mcc – microcline, Ntr – natrolite, Pgdn – plumbogaidonnayite.

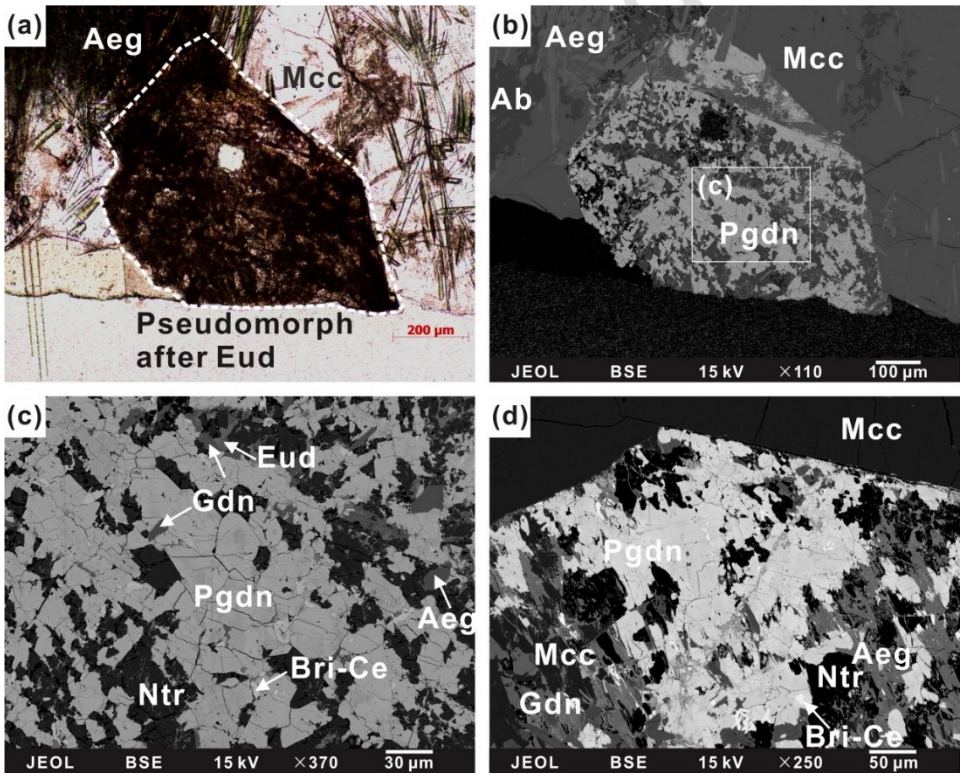

DOI: 10.1180/mgm.2024.2

Fig. 2. The Raman spectrum for plumbogaidonnayite.

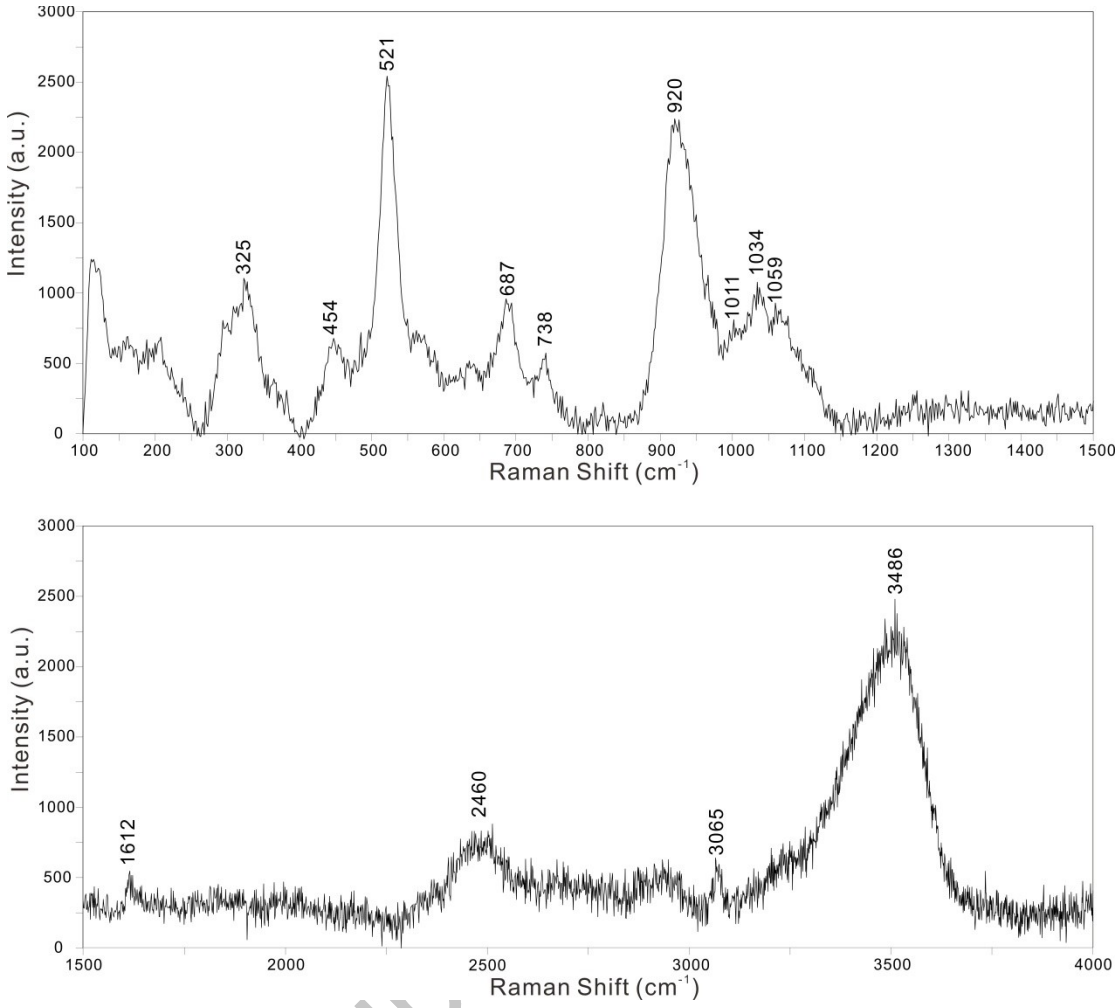

https://doi.org/10.1180/mgm.2024.2 Published online by Cambridge University Press

Fig. 3. Compositional variations for plumbogaidonnayite plotted on Pb *vs.* Ca + (Na+K)/2 diagram.

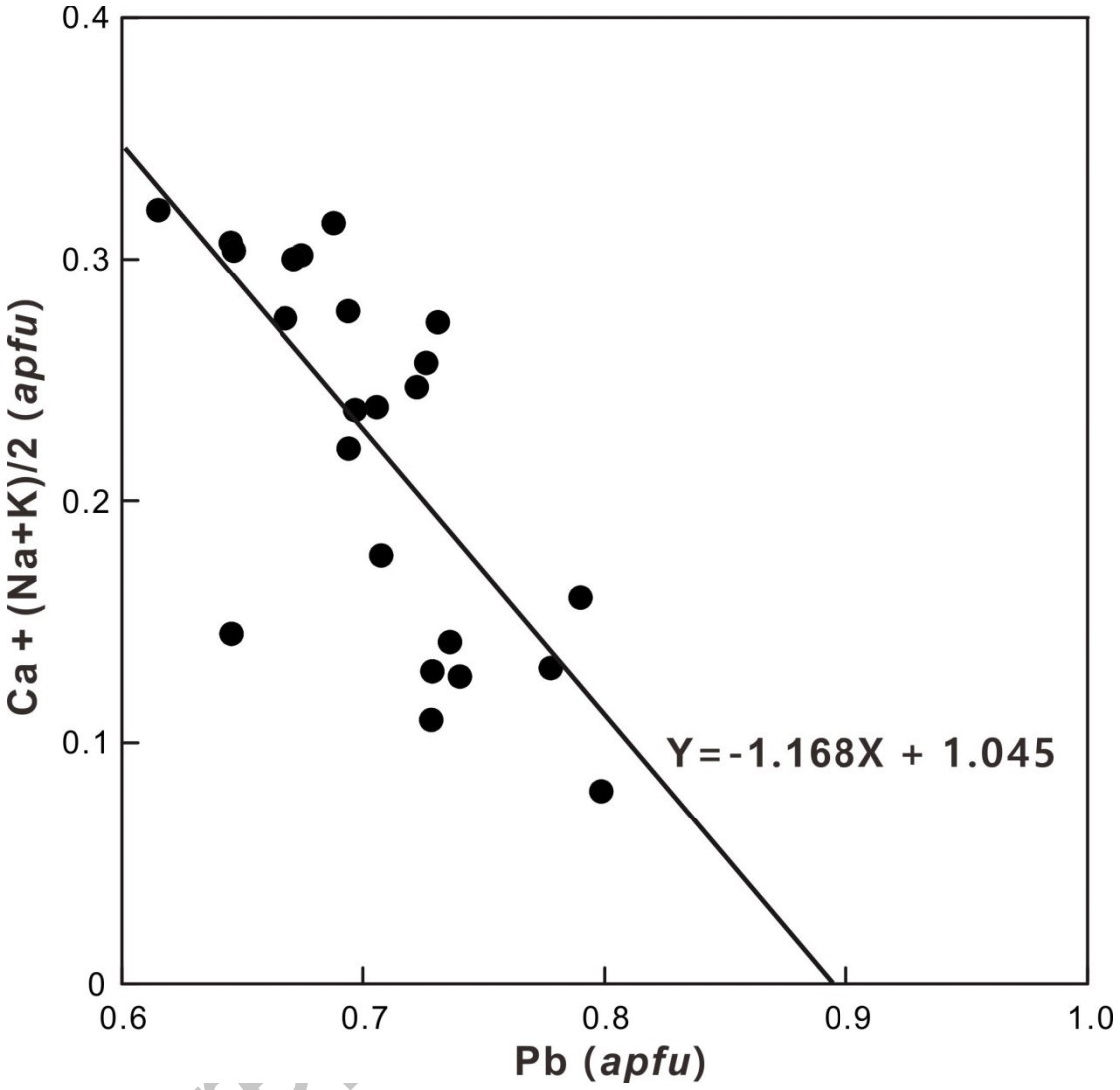

https://doi.org/10.1180/mgm.2024.2 Published online by Cambridge University Press

Fig. 4. Crystal structure of plumbogaidonnayite (unit cell outlined in black lines) plotted with VESTA 3 (Momma and Izumi, 2011). (a) The sinusoidal six [SiO_4] tetrahedra-repeat single silicate chain. (b) ZrO_6 octahedra and SiO_4 tetrahedra form 7-member ring and 3-member ring from the view along the *c*-axis. (c) Disordered Pb (Pb1, Pb2 and Pb3), Ca (Ca1, K1 and Pb4) and two H_2O groups (O10 and O11) distribute over the space between the ZrO_6-SiO_4 framework (modified after Wu *et al.*, 2023c).

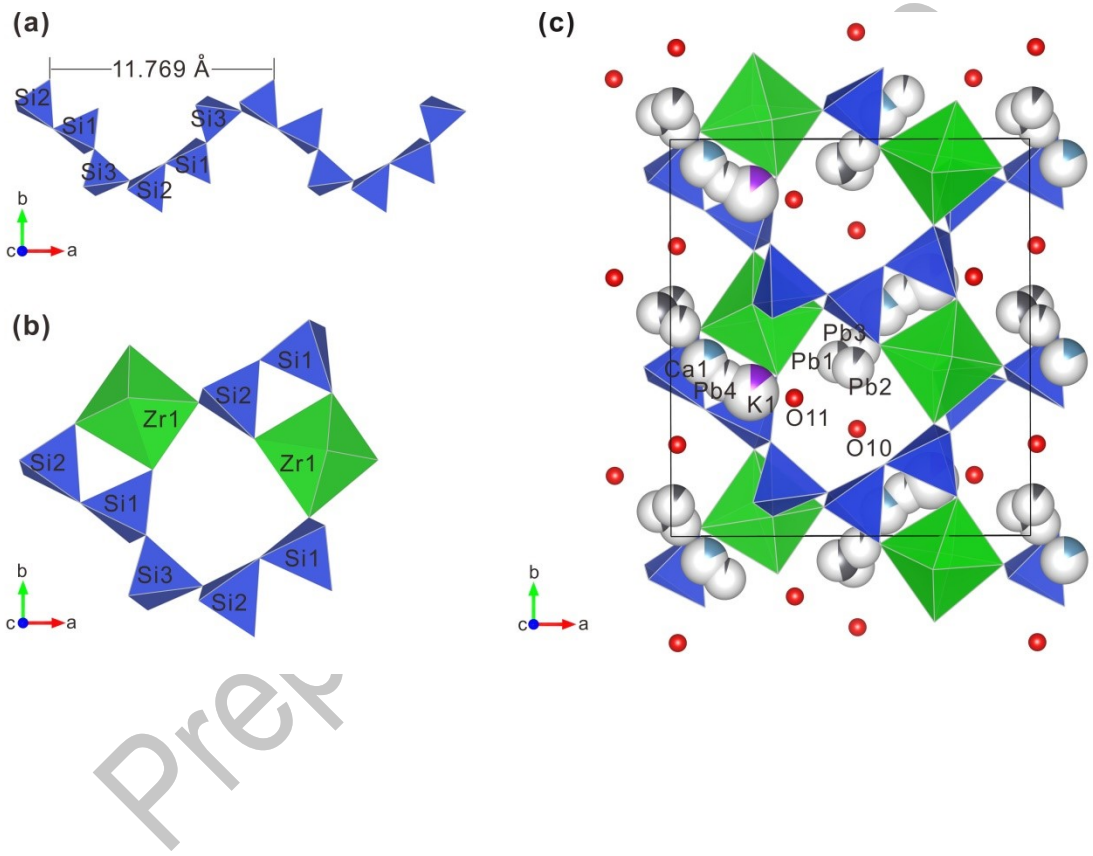

https://doi.org/10.1180/mgm.2024.2 Published online by Cambridge University Press